Polymer 51 (2010) 2508–2514

Contents lists available at ScienceDirect

Polymer

journal homepage: www.elsevier.com/locate/polymer

Castor oil-based thermosets with varied crosslink densities prepared by ring-opening metathesis polymerization (ROMP)

Ying Xia, Richard C. Larock*

Department of Chemistry, Iowa State University, Ames, IA 50011, USA

ARTICLE INFO

Article history:
Received 17 February 2010
Received in revised form
2 April 2010
Accepted 8 April 2010
Available online 18 April 2010

Keywords:
Castor oil
ROMP
Crosslink density

ABSTRACT

Two castor oil-based monomers, (1) norbornenyl-functionalized castor oil (NCO), which has ~0.8 norbornene rings per fatty acid chain and (2) norbornenyl-functionalized castor oil alcohol (NCA), which has ~1.8 norbornene rings per fatty acid chain, have been prepared. Ring-opening metathesis polymerization (ROMP) of different ratios of NCO/NCA using the 2nd generation Grubbs catalyst results in rubbery to rigid biorenewable-based plastics with crosslink densities ranging from 318 to 6028 mol/m^3. Increased crosslink densities result in shorter gelation times, better incorporation of the monomers into the polymer network, and much less soluble materials in the bulk materials. The increased crosslink densities obtained by adding NCA enhance the thermal properties, including the glass transition temperature (T_g) and room temperature storage modulus, which increase from −17.1 °C to 65.4 °C and from 2.4 MPa to 831.9 MPa, respectively. The TGA results, where T_{10} increased from 285 °C to 385 °C, illustrate that improved thermal stabilities can be obtained for thermosets with higher crosslink densities. Young's modulus (11–407 MPa), tensile strength (1.6–18 MPa) and toughness (0.14–1.6 MPa) are also improved dramatically with higher crosslink densities.

Published by Elsevier Ltd.

1. Introduction

Bioplastics derived from vegetable oils represent a promising route to green materials, because of the ready availability of the oils and the inherent biodegradability of the products [1]. A variety of biorenewable materials, including thermosetting resins [2–4], thermoplastics [5] and biocomposites [6–8], suitable for the replacement of petroleum-based materials have been prepared from vegetable oils and their derivatives. Castor oil's unique structure, where ~90% of the fatty acid chains bear an hydroxyl group, makes it a very useful vegetable oil in industry [9]. A wide variety of polymers, especially polyurethanes [10], have been prepared by taking advantage of the hydroxyl groups.

Olefin metathesis, which is a relatively new polymerization method [11], has been employed to prepare vegetable oil-based polymers. For example, recently, acyclic diene (triene) metathesis polymerization (ADMET/ATMET) has been used to prepare plant oil-based polymers [12]. Novel biorenewable materials have been prepared by ring-opening metathesis polymerization (ROMP) as well. For example, two kinds of ROMP-based systems, norbornenyl anhydride-functionalized castor oil (BCO)/cyclooctene (CO) [13] and Dilulin (a norbornenyl-functionalized linseed oil [14])/dicyclopentadiene (DCPD) [15], have been developed in our group previously. Both systems afford green thermosets and provide a promising new route to bioplastics from biorenewable resources.

However, some improvements need to be made to obtain better ROMP bioplastics. In the BCO/CO system, pure BCO does not undergo facile ROMP because the free carboxylic groups result in strong hydrogen bonding, which hinders coordination between the olefin and the catalyst [13]. In addition, a relatively high loading of the Grubbs catalyst (0.5 wt%) was required to afford good polymers. For the Dilulin/DCPD system, phase separations were clearly observed due to the difference in ROMP reactivity between DCPD and Dilulin, where approximately two thirds of the fatty acid side chains are not appended with norbornene rings.

To address previously mentioned problems and prepare better ROMP systems, two castor oil-based monomers, (1) norbornenyl-functionalized castor oil (NCO), which has ~0.8 norbornene rings per fatty acid chain and (2) norbornenyl-functionalized castor oil alcohol (NCA), which has ~1.8 norbornene rings per fatty acid chain, have been prepared for ROMP. Mixtures of NCO and NCA in different ratios have been polymerized using only 0.125 wt% of the 2nd generation Grubbs catalyst, resulting in novel castor oil-based rubbery to rigid biorenewable plastics with crosslink densities ranging from 318 to 6028 mol/m^3. The thermal and mechanical analysis results indicate that higher T_gs, higher storage moduli,

* Corresponding author. Tel.: +1 5152944660; fax: +1 5152940105.
E-mail address: larock@iastate.edu (R.C. Larock).

0032-3861/$ – see front matter Published by Elsevier Ltd.
doi:10.1016/j.polymer.2010.04.014

better thermal stabilities and improved mechanical properties are obtained for the thermosets with higher crosslink densities.

2. Experimental section

2.1. Materials

Castor oil, acryloyl chloride, triethylamine and the 2nd generation Grubbs catalyst were purchased from Sigma–Aldrich (Milwaukee, WI). Dicyclopentadiene (DCPD) (>95% pure) was purchased from Alfa Aesar (Ward Hill, MA). Lithium aluminum hydride (LAH) was purchased from Acros (Geel, Belgium). Benzene, ethyl acetate, methylene chloride, $NaHCO_3$ and HCl were obtained from Fisher (Fair Lawn, NJ). Tetrahydrofuran (THF) was distilled over sodium/benzophenone under N_2. Unless otherwise stated, all reagents were used as received without further purification.

2.2. Synthesis of bicyclo[2.2.1]hept-2-ene-5-carbonyl chloride [16]

Freshly cracked cyclopentadiene (56 g, 0.85 mol) was added dropwise to a solution of acryloyl chloride (70 g, 0.77 mol) in toluene (275 mL) at 0 °C. The reaction was run at 0 °C for 3 h and then heated to 100 °C and held at that temperature for 0.5 h. The toluene was distilled off and the residual liquid was distilled under reduced pressure to yield 95 g (79%) of the product as a clear and colorless oil (83:17 *endo*:*exo*). ^{1}H NMR ($CDCl_3$, δ ppm) at 1.31–1.34 (d), 1.47–1.52 (m), 1.90–1.94 (m), 2.70–2.73 (m), 2.97 (s), 3.27 (s), and 3.43–3.47 (m) are assigned to the non-olefinic protons of both the *endo* and *exo* isomers; 6.02 (m, =CH, *endo*), 6.12 (m, =CH, *exo*), 6.20 (m, =CH, *exo*), 6.25 (m, =CH, *endo*).

2.3. Synthesis of norbornenyl-functionalized castor oil (NCO)

Scheme 1 (path a) illustrates the preparation of NCO. Castor oil (20 g, 0.021 mol) was dissolved in 100 mL of anhydrous CH_2Cl_2 and cooled to 0 °C. A solution of bicyclo[2.2.1]hept-2-ene-5-carbonyl chloride (10.6 g, 0.068 mol) in 100 mL of anhydrous CH_2Cl_2 was added dropwise and then triethylamine (11.4 g, 0.11 mol) was added. The solution was stirred, while allowing it to warm from 0 °C to room temperature, and was maintained at that temperature for 48 h. Then the reaction mixture was stirred with 500 mL of aqueous 5 wt% Na_2CO_3 solution overnight to convert the excess bicyclo[2.2.1]hept-2-ene-5-carbonyl chloride to the corresponding water soluble carboxylate salt. After extraction with CH_2Cl_2 and removal of the solvent, a quantitative yield of NCO was obtained as a brown liquid. Fig. 1(b) shows the ^{1}H NMR peak assignments for NCO, which contains ~0.8 norbornene rings per fatty acid chain as determined by ^{1}H NMR spectral analysis.

2.4. Synthesis of norbornenyl-functionalized castor oil alcohol (NCA)

The preparation of NCA is illustrated in Scheme 1 (path b). LAH (12.27 g, 0.32 mol) was added to 100 mL of THF and stirred in a 1000 mL two-neck round bottom flask at 0 °C. Castor oil (100 g, 0.11 mol) was dissolved in 600 mL of THF and then added dropwise to the LAH suspension. The reaction was maintained at 0 °C overnight. The reaction mixture was poured into ice water, followed by the addition of 1 M HCl, until the solution was clear. Then 300 mL of ethyl acetate was added to carry out the extraction. The organic layer was washed with water to remove glycerol, dried over $MgSO_4$ and filtered. Finally, the clear castor oil alcohol was obtained after removal of the organic solvent under vacuum.

Castor oil alcohol (20 g, 0.071 mol) was dissolved in 100 mL of anhydrous CH_2Cl_2 and cooled to 0 °C. A solution of bicyclo[2.2.1]hept-2-ene-5-carbonyl chloride (22.73 g, 0.15 mol) in 100 mL of anhydrous CH_2Cl_2 was added dropwise and then triethylamine (14.68 g, 0.15 mol) was added. The solution was stirred, while allowing it to warm from 0 °C to room temperature, and was maintained for 24 h at that temperature. Then the reaction mixture was stirred with 500 mL of aqueous 5 wt% Na_2CO_3 solution overnight to convert the excess bicyclo[2.2.1]hept-2-ene-5-carbonyl

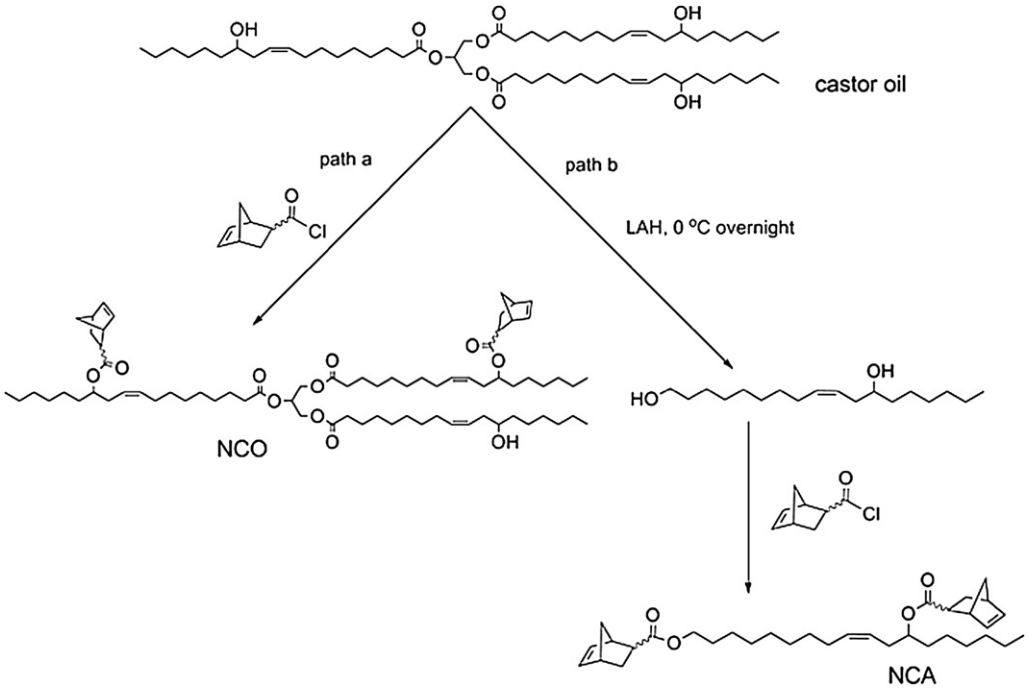

Scheme 1. Preparation of NCO (path a) and NCA (path b) from castor oil.

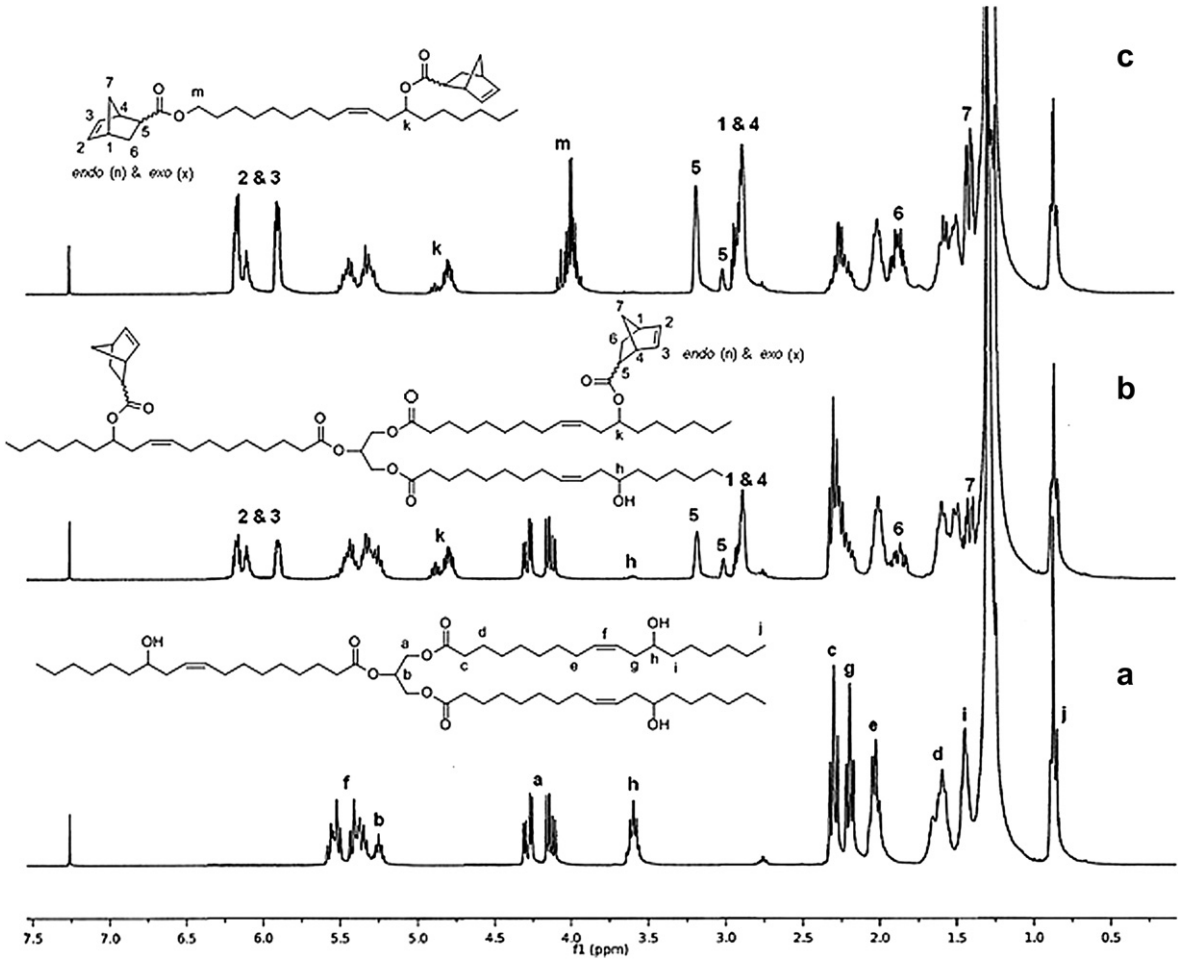

Fig. 1. Structures and ^{1}H NMR spectra of (a) castor oil, (b) norbornenyl-functionalized castor oil (NCO) and (c) norbornenyl-functionalized castor oil alcohol (NCA).

chloride to a water soluble carboxylate salt. After extraction with CH_2Cl_2 and removal of the solvent, a quantitative yield of NCA with a light brown color was obtained. Fig. 1(c) shows the ^{1}H NMR peak assignments for NCO, which contains ~1.8 norbornene rings per fatty acid chain as determined by ^{1}H NMR spectral analysis.

2.5. Freeze-drying of the Grubbs catalyst

To improve the solubility of the Grubbs catalyst in the monomers, freeze-drying of the catalyst was carried out according to a literature procedure [17]. The 2nd generation Grubbs catalyst (250 mg) was dissolved in 5 mL of benzene and the solution was frozen in a liquid nitrogen bath. The frozen sample was then placed in a vacuum oven at room temperature for 5 h to sublime the benzene. This process provided catalyst with a larger surface area.

2.6. Polymerization

Freeze-dried Grubbs 2nd generation catalyst (5 mg, 0.125 wt%) was dissolved in the mixture of NCO and NCA (4 g) and stirred with a spatula until all of the catalyst was dissolved and a homogeneous solution was obtained. The solution was poured into a glass mold and cured at 65 °C for 1 h and 150 °C for 3 h. The resulting thermosets were transparent, but retain the monomers' original color.

2.7. Soxhlet extractions

A 1.5 g sample of the bulk polymer was extracted with 100 mL of refluxing methylene chloride for 24 h using a Soxhlet extractor. Following extraction, the resulting solution was concentrated under reduced pressure and dried in a vacuum oven at 60 °C overnight.

2.8. Characterization

^{1}H NMR spectroscopic analysis of the monomers and the soluble substances extracted from the thermosets by methylene chloride were recorded in $CDCl_3$ using a Varian spectrometer (Palo Alto, CA) at 300 MHz.

The gelation time was determined on an AR2000ex by applying an oscillating strain to the sample and measuring the response stress. All experiments were performed at 50 °C with the stress control mode at 1 Hz using 25-mm diameter disposable parallel plates and a 0.5 mm gap.

The dynamic mechanical analyses (DMA) were recorded on a TA Instruments Q800 dynamic mechanical analyzer using a film tension mode of 1 Hz. Rectangular samples 0.77 mm thick and 8 mm wide were used for the analysis. The samples were cooled and held isothermally for 3 min at −80 °C before the temperature was increased at 3 °C/min to 200 °C.

Thermogravimetric analysis (TGA) of the specimens was carried out on a TA Instruments (New Castle, DE) Q50. The samples were scanned from 50 °C to 650 °C in air at a heating rate of 20 °C/min.

The mechanical properties of the thermosets were determined using an Instron universal testing machine (model 4502) with a crosshead speed of 50 mm/min. Rectangular specimens of $70 \times 8 \times 0.8$ mm^3 (length × width × thickness) were used. An average value of four replicates of each sample was taken. The toughness of the polymer, which is the fracture energy per unit volume of the sample, was obtained from the area under the corresponding tensile stress–strain curves.

3. Results and discussion

3.1. Synthesis of the monomers

Castor oil is a vital industrial oil with a typical triglyceride structure containing ~90% ricinoleic acid chains [9]. A representative structure and ^{1}H NMR spectrum of castor oil are shown in Fig. 1(a). The signals at 4.1–4.4 ppm (a) correspond to the methylene protons in the glyceride unit. The vinyl protons (*f*) in the fatty acid chains are observed at 5.3–5.6 ppm. The tertiary hydrogens adjacent to the hydroxyl group in the fatty acid chain (*h*) are detected at 3.6 ppm. The detailed peak assignments are listed in Fig. 1(a).

The hydroxyl groups of the fatty acid chains make modification of the castor oil quite easy. Esterification of the castor oil by bicyclo[2.2.1]hept-2-ene-5-carbonyl chloride proceeds easily and the norbornenyl-functionalized monomer NCO can be obtained in an excellent yield. Fig. 1(b) shows the structure of NCO and the ^{1}H NMR spectral peak assignments. Compared to castor oil, peak *h* is substantially reduced in NCO, which means that most of the hydroxyl groups have reacted and a new peak representing the tertiary hydrogen adjacent to the norbornenyl ester is observed at 4.8 ppm. By integrating the peaks *k* and *h*, it was found that ~95% of the hydroxyl groups reacted with bicyclo[2.2.1]hept-2-ene-5-carbonyl chloride and approximately 2.4 norbornene rings were incorporated into the triglyceride (0.8 norbornene rings per fatty acid chain). Besides the peaks corresponding to the castor oil, norbornene hydrogens are found at 5.9–6.2 ppm. The other non-olefinic norbornenyl hydrogens are assigned as well.

To prepare a monomer with more norbornene rings per fatty acid chain, castor oil has been reduced to castor oil alcohol (mainly ricinoleic alcohol), which was then reacted with bicyclo[2.2.1]hept-2-ene-5-carbonyl chloride to prepare NCA (Scheme 1 – path b). Fig. 1(c) illustrates the structure and ^{1}H NMR spectra of NCA. Compared to castor oil in Fig. 1(a), the peaks *a* and *h* disappear, which indicates that castor oil's triglyceride structure was reduced completely and all of the hydroxyl groups were reacted with bicyclo[2.2.1]hept-2-ene-5-carbonyl chloride. A new peak *m* represents the methylene protons adjacent to the norbornenyl ester. Based on the integration of peaks *k* and *m*, it was found that NCA contains approximately 1.8 norbornene rings per fatty acid chain, which is about 2.3 times the number of norbornene rings present in NCO.

3.2. ROMP of NCO and NCA

Taking advantage of the high reactivities of the strained norbornene rings appended to NCO and NCA, ROMP readily copolymerizes these two castor oil-based monomers. Scheme 2 illustrates the copolymerization of NCO and NCA. The amount of catalyst used and the cure sequence employed are based on previous research in our group [15]. Thermosets containing 0–100 wt% of NCO at 20 wt% intervals were prepared. Because NCA (~1.8 norbornene rings per fatty acid chain) was copolymerized with NCO (~0.8 norbornene rings per fatty acid chain) in various ratios, thermosets with different crosslink densities can be obtained. Table 1 summarizes the amount of soluble materials obtained from methylene chloride Soxhlet extraction of these thermosets. As one can see from the table, the soluble fraction decreases from 27.7 wt% to 0.8 wt% as the

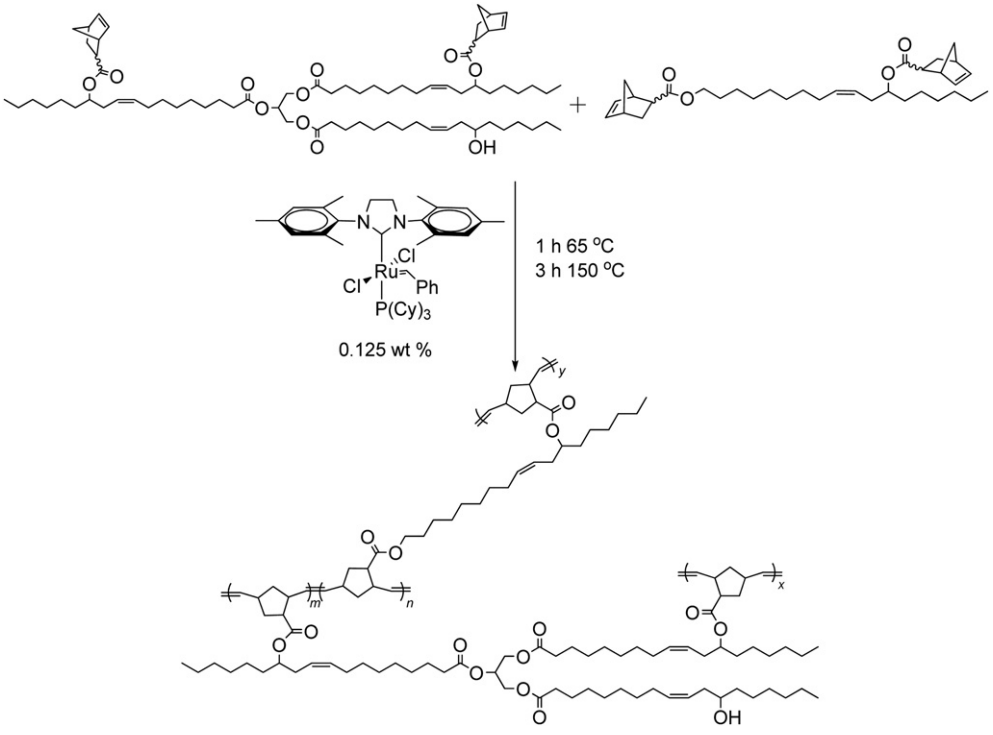

Scheme 2. ROMP of NCO and NCA.

Table 1
Extraction data, gelation times and DMA data for the polymers.

Polymer	Soluble fraction (%)	Gel time/s[a]	T_g (°C)[b]	υ_e (mol/m^3)[c]	(Tan δ)$_{max}$	E' at 25 °C (MPa)
NCO100	27.7	3704	−17.1	318	1.21	2.4
NCO80NCA20	14.7	2611	−6.2	740	0.81	5.7
NCO60NCA40	6.7	1617	14.6	1664	0.46	27.8
NCO40NCA60	2.5	1525	27.5	2790	0.42	130.0
NCO20NCA80	1.0	431	49.1	4418	0.32	583.4
NCA100	0.8	34	65.4	6028	0.27	831.9

[a] The gelation time was determined at 50 °C.
[b] Glass transition temperatures represent the maxima of the tan δ curves obtained by DMA analysis.
[c] Crosslink densities have been calculated at temperatures 50 °C above the T_g.

NCA amount increases from 0 to 100%. This can be explained by the fact that more crosslinked insoluble polymer network is formed with more NCA, which has a larger norbornene ring density.

The gelation time was determined for all NCO/NCA copolymers using a reported rheology procedure [18]. In general, the viscosity of the monomer/catalyst dramatically increases when gelation occurs. A parallel plate oscillatory rheometer was used to determine the time dependence of the storage shear modulus, G', and the loss shear modulus, G'', for the various monomer/catalyst mixtures. All gelation experiments were performed at 50 °C to make sure appropriate gelation times were obtained for all samples. Fig. 2 illustrates the increase in both G' and G''. The gelation time was obtained when G' crosses over G'', which indicates the transition of the system from liquid phase dominated to a solid phase dominated viscoelastic behavior with a three-dimensional (3-D) network formation [19]. Table 1 summarizes the gelation times for all of the samples. As seen from the table, the addition of NCA decreases the gelation time for the NCO/NCA system. NCA is so effective that the gelation time was decreased from 3704 s to 34 s, when the NCA amount increases from 0 to 100%. As mentioned above, the gelation time represents the moment when a crosslinked 3-D network is formed. The amount of NCA present, which has more crosslink sites per fatty acid chain, accelerates formation of the crosslinked network and decreases the gelation time.

3.3. Thermal properties

Fig. 3 shows the storage modulus (E') and tan δ curves as a function of temperature for different NCO/NCA ratios. Only one peak was observed in the tan δ versus T curves for all of the copolymers, which indicates that they are homogeneous copolymers. All thermosets are in the glassy state at low temperatures and E' decreases slightly when the temperature increases. Then a rapid decrease in the E' value is observed for all of the thermosets in the temperature range of −25 to 100 °C, which is due to the primary relaxation process (α) of the NCO/NCA copolymers obtained, where a maximum is observed in the tan δ versus T curve and the temperature there is taken as the glass transition temperature (T_g). At high temperatures after the α relaxation, a plateau was observed in the E' versus T curves, which is evidence for the existence of the crosslinked network in the NCO/NCA thermosets. The crosslink density (ν_e) of all of the copolymers can be determined from the rubbery moduli using the following equation, according to the kinetic theory of rubber elasticity [20,21]:

$$E' = 3\nu_e RT$$

where E' is the storage modulus at $T_g + 50$ °C in the rubbery plateau, R is the gas constant, and T is the absolute temperature at $T_g + 50$ °C. As one can see from Table 1, the crosslink density increases dramatically from 318 to 6028 mol/m^3, when the NCA amount increases from 0 to 100%. This indicates that increasing the amount of NCA in the copolymers results in a more crosslinked network, which enhances the thermosets' rubbery modulus. The glass transition temperatures (T_gs), (tan δ)$_{max}$ values and room temperature storage moduli (E' at 25 °C) for all of the copolymers

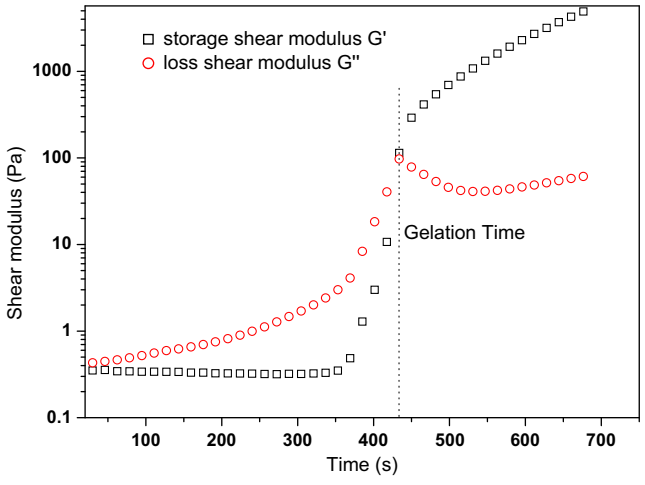

Fig. 2. Evolution of the shear moduli during the cure process. Shown here is the NCO20NCA80/catalyst mixture curing at 50 °C.

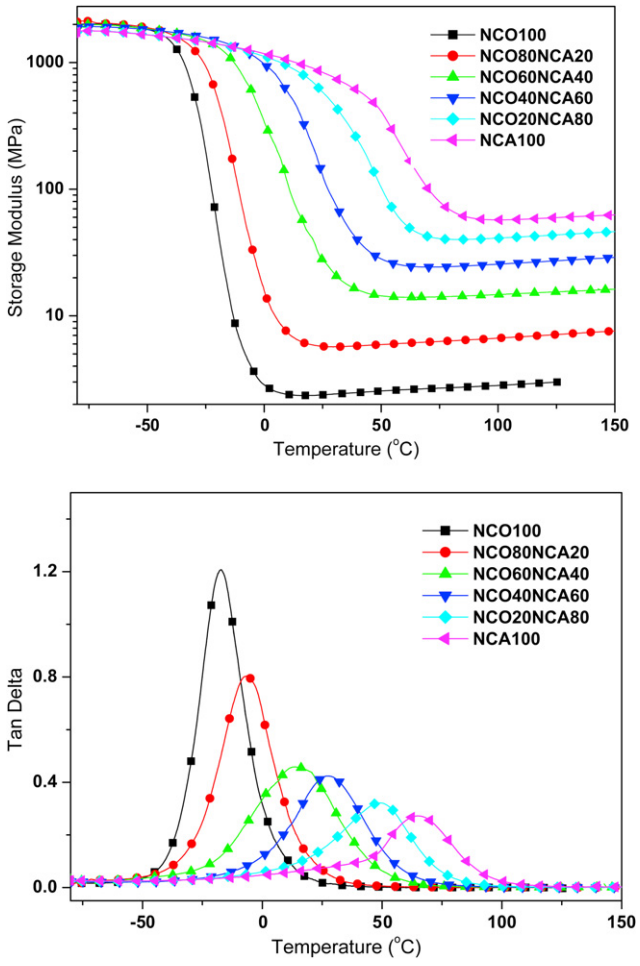

Fig. 3. Storage modulus and tan δ curves for all polymers.

are also summarized in Table 1. As the crosslink density increases with an increase in the NCA amount, molecular motions become more restricted and the amount of energy that can be dissipated throughout the polymer specimen decreases dramatically. Therefore, the tan δ peak shifts to a higher temperature and the $(\tan\delta)_{max}$ decreases when the NCA amount increases. Meanwhile, the room temperature storage modulus is enhanced considerably by increasing the NCA content in the thermosets.

The T_gs of all copolymers are in the range of −17.1 to 65.4 °C, which indicates that rubbery to rigid plastics are obtained by changing the NCO/NCA ratio. Fig. 4 shows the dependence of the T_gs of the NCO/NCA copolymers on the NCA content. A square indicates the T_gs obtained from experiment and how they increase linearly with an increase in the NCA content. Round dots indicate the T_gs calculated based on the Fox equation:

$$\frac{1}{T_g} = \frac{w_a}{T_{g,a}} + \frac{w_b}{T_{g,b}}$$

where $T_{g,a}$ and $T_{g,b}$ represent the glass transition temperatures of polyNCO and polyNCA and w_a and w_b are their mass fractions. As we can see from Fig. 4, the experimental T_gs fit very well with the calculated T_gs. The linear increase of T_gs clearly indicates that the increase in NCA content increases the glass transition temperatures due to better incorporation of the monomers into the copolymer network with resulting higher crosslink densities. Similar results have been reported by Sheng et al. previously [22].

The TGA analysis of all copolymers is shown in Fig. 5 and all of the corresponding data (T_{10}, T_{50} and T_{max}) are summarized in Table 2. As seen from Fig. 5, all thermosets are stable up to 200 °C and three decomposition stages are clearly seen. The first stage from 200 °C to 425 °C corresponds to evaporation and decomposition of the unreacted monomers and other soluble materials in the bulk materials [23]. The weight percentage lost in the first stage decreases for thermosets with higher NCA content, which is due to more effective crosslinking in the polymer. The second stage (425–475 °C) is the fastest degradation stage. It represents decomposition of the polymer backbone in the bulk thermosets. The last stage (>475 °C) corresponds to further oxidation of the crosslinked network and gradual oxidation of the char residue. It can be seen from Table 2 that T_{10}, T_{50} and T_{max} for all of the copolymers increase with an increase in the NCA content. This can be explained by the fact that increased crosslink densities improve the thermal stabilities of the final thermosets.

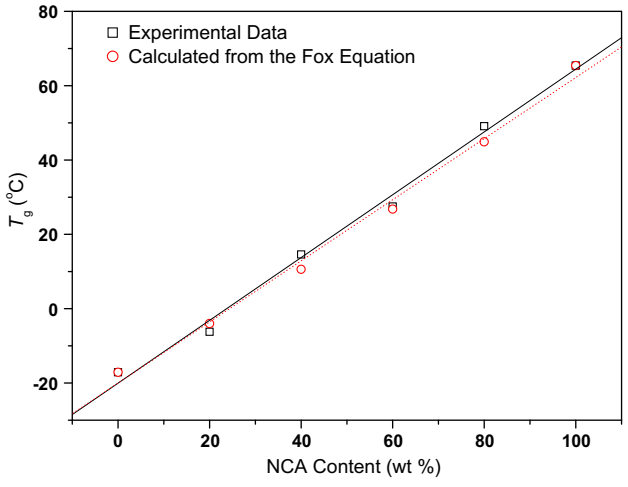

Fig. 4. The dependence of glass transition temperature (T_g) of the NCO/NCA copolymers on the NCA content.

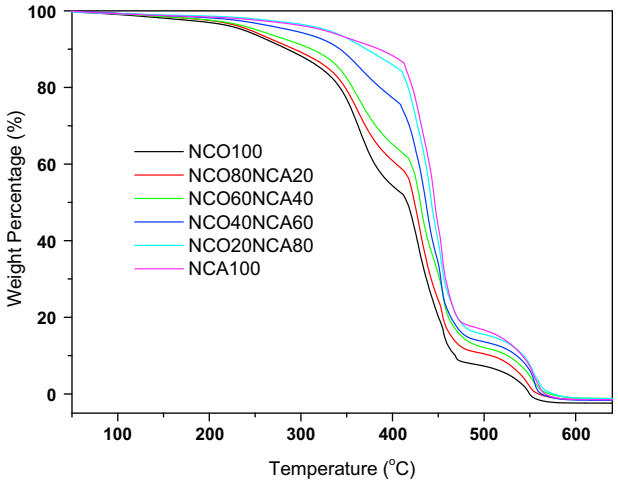

Fig. 5. TGA curves for all NCO/NCA copolymers.

3.4. Mechanical properties

Fig. 6 shows the tensile stress–strain behavior of several NCO/NCA copolymers and Table 2 summarizes their Young's moduli, tensile strengths, elongation at break values, and toughness. PolyNCO100 and polyNCO80NCA20 are too weak to run the tensile tests; so only the other four samples have been investigated. The NCO/NCA copolymers exhibit a variety of stress–strain behaviors depending on the amount of NCA used. PolyNCO60NCA40 and polyNCO40NCA60 exhibit behavior as weak and ductile plastics with Young's moduli of 11.0 and 25.7 MPa, respectively. Much better mechanical properties are observed when the NCA amount is increased to 80 and 100%; polyNCO20NCA80 and polyNCA100 show Young's moduli of 166.6 and 407 MPa, and ultimate tensile strengths of 8.9 and 18.0 MPa respectively, which are dramatically enhanced compared to the analogous properties for polyNCO60NCA40 and polyNCO40NCA60. The improvements can be explained by both an increase in the crosslink density and the rigidity of the thermosets. Besides the higher crosslink densities obtained when using more NCA, the number of rigid cyclopentane rings obtained after ring-opening of the norbornene rings increases with an increase in the NCA content. In addition to Young's moduli and tensile strengths, toughness values have also been obtained from the stress–strain curves by integrating the areas under the stress–strain curves. Tensile toughness is a materials' resistance to fracture when stressed and both the tensile strength and the elongation at break contribute to the tensile toughness. As seen from Table 2, the tensile toughness increases with an increase in the NCA content as well.

Table 2
TGA data and mechanical properties for the polymers.

Polymer	TGA data (°C)			Mechanical properties[d]			
	T_{10}[a]	T_{50}[b]	T_{max}[c]	E (MPa)	σ_b (MPa)	ε_b (%)	Toughness (MPa)
NCO100	285	416	429	–	–	–	–
NCO80NCA20	293	424	429	–	–	–	–
NCO60NCA40	312	430	431	11.0 ± 0.4	1.6 ± 0.2	16.3 ± 2.9	0.14 ± 0.04
NCO40NCA60	343	436	437	25.7 ± 2.5	4.5 ± 0.2	25.2 ± 0.5	0.6 ± 0.02
NCO20NCA80	372	443	441	166.6 ± 9.3	8.9 ± 0.7	15.6 ± 2.1	0.9 ± 0.2
NCA100	385	446	445	407.0 ± 37	18.0 ± 0.4	13.0 ± 3.9	1.6 ± 0.6

[a] 10% Weight loss temperature.
[b] 50% Weight loss temperature.
[c] Temperature of maximum thermal degradation.
[d] E = Young's modulus, σ_b = tensile strength, and ε_b = elongation at break.

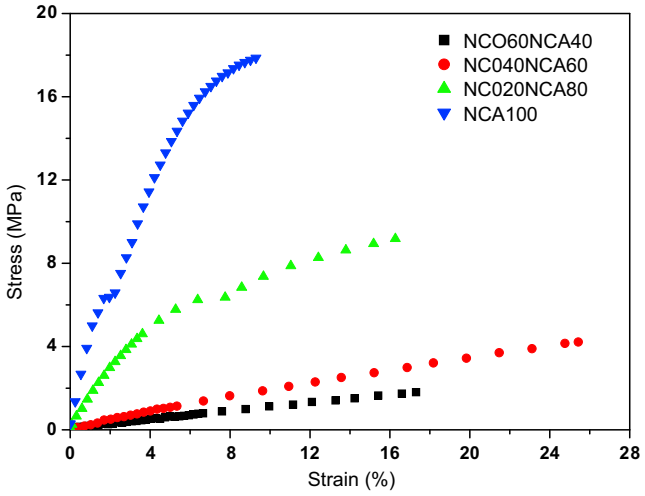

Fig. 6. Tensile stress–strain curves for several NCO/NCA copolymers.

4. Conclusions

Two castor oil-based ROMP monomers, NCO and NCA, which have different numbers of norbornene rings per fatty acid side chain have been prepared and bioplastics with different crosslink densities ranging from 318 to 6028 mol/m^3 have been obtained by varying the initial NCO/NCA ratio during ROMP. The amount of soluble materials obtained by extraction of the NCO/NCA copolymers decreases considerably as the NCA content increases, because of increased crosslinking. The gelation times also dramatically decrease as the NCA content increases. The thermal properties, namely the T_gs and room temperature storage moduli, are improved with an increase in the NCA content. The T_gs increase linearly with the amount of NCA and fit well with the data calculated based on the Fox equation. The TGA data reveals that the thermosets with higher crosslink densities have better thermal stabilities. In addition, the mechanical properties, namely Young's moduli, tensile strength and toughness, are also improved with an increase in NCA content. These castor oil-based thermosets represent another promising route to environmentally friendly plastics.

Acknowledgment

We are grateful for financial support from the Center for Crops Utilization Research (CCUR) at Iowa State University and thankful to Professor Michael Kessler in the Department of Materials Science and Engineering at Iowa State University for the use of his thermal analysis equipment. In addition, we thank Dr. Yongshang Lu for his thoughtful discussions.

References

[1] Lu YS, Larock RC. ChemSusChem 2009;2:136–47.
[2] Montero de Espinosa L, Ronda JC, Galia M, Cadiz V. J Polym Sci Part A Polym Chem 2009;47:4051–63.
[3] Montero de Espinosa L, Ronda JC, Galia M, Cadiz V. J Polym Sci Part A Polym Chem 2009;47:1159–67.
[4] Montero de Espinosa L, Ronda JC, Galia M, Cadiz V. J Polym Sci Part A Polym Chem 2008;46:6843–50.
[5] Tian HF, Liu DG, Zhang L. J Appl Polym Sci 2009;111:1549–56.
[6] Liu WJ, Misra M, Askeland P, Drzal LT, Mohanty AK. Polymer 2005;46:2710–21.
[7] Quirino RL, Larock RC. J Appl Polym Sci 2009;112:2033–43.
[8] Pfister DP, Baker JR, Henna PH, Lu Y, Larock RC. J Appl Polym Sci 2008;108:3618–25.
[9] Ogunniyi DS. Bioresour Technol 2006;97:1086–91.
[10] Sharma V, Kundu PP. Prog Polym Sci 2008;33:1199–215.
[11] Trnka TM, Grubbs RH. Acc Chem Res 2001;34:18–29.
[12] Meier MAR. Macromol Chem Phys 2009;210:1073–9.
[13] Henna PH, Larock RC. Macromol Mater Eng 2007;292:1201–9.
[14] Kodali DR. U.S. Patent 6420322; 2002.
[15] Henna P, Larock RC. J Appl Polym Sci 2009;112:1788–97.
[16] Arehart SV, Pugh C. J Am Chem Soc 1997;119:3027–37.
[17] Jones AS, Rule JD, Moore JS, White SR, Sottos NR. Chem Mater 2006;18:1312–7.
[18] Sheng X, Lee JK, Kessler MR. Polymer 2009;50:1264–9.
[19] Weng LH, Chen XM, Chen WL. Biomacromolecules 2007;8:1109–15.
[20] Flory PJ. Principles of polymer chemistry. Ithaca: Cornell Univerisity Press; 1953.
[21] Ward IM. Mechanical properties of solid polymers. New York: Wiley Interscience; 1971.
[22] Sheng X, Kessler MR, Lee JK. J Therm Anal Calorim 2007;89:459–64.
[23] Andjelkovic DD, Larock RC. Biomacromolecules 2006;7:927–36.